

Effect of antiangiogenic targeted chemotherapy on the osseointegration of titanium implants in rabbits

B. Al-Jandan

Biomedical Dental Sciences Department, College of Dentistry, Imam Abdulrahman Bin Faisal University, Dammam, Saudi Arabia

Accepted 9 January 2019

Available online 22 January 2019

Abstract

Patients with cancer have recently been treated with more advanced targeted chemotherapies that have greater specificity towards the cancer cells and fewer side effects. However, the periods of treatment take longer than those of traditional cytotoxic treatments. The aim of this study was to examine the effect of antiangiogenic targeted chemotherapy on the osseointegration of titanium implants. Fourteen white New Zealand rabbits were allocated randomly into two groups of seven: the placebo control group and the Avastin[®] group. Animals in the Avastin[®] group had five doses of bevacizumab intraperitoneally (3 mg/kg/week). The first was given two days before the implant was inserted and the remaining four were given weekly for four weeks. One titanium implant was inserted in the right distal femoral condyle of each rabbit. Osseointegration of the implants was measured using microcomputed tomography (CT) and histomorphometric evaluation. Both of these showed less osseointegration in the Avastin[®] group than in the controls. The pharmacological inhibition of angiogenesis by bevacizumab may negatively affect the osseointegration of titanium implants in rabbits.

© 2019 Published by Elsevier Ltd on behalf of The British Association of Oral and Maxillofacial Surgeons.

Keywords: dental implants; targeted chemotherapy; anti-angiogenesis; bevacizumab; Avastin; osseointegration

Introduction

Recent advances in dental implants have led to an increase in the number of patients treated, with survival rates of more than 95% in a healthy population.¹ Chemotherapy aims to stop the growth, invasion, and metastasis of cancer cells. As traditional agents mainly affect proliferation, which is a characteristic of cancer cells as well as normal cells, normal tissues with a high rate of turnover (such as mucous membranes and bone marrow) can also be adversely affected.² Late side effects of traditional (non-targeted) chemotherapy include malnutrition of bone and diminished remodelling.³ Al-Mahalawy et al found that cisplatin (a

traditional chemotherapeutic agent) markedly inhibited the osseointegration of titanium implants.⁴

The lack of selectivity for tumour cells by chemotherapy may lead to drug resistance or result in systemic toxicity.⁵ Recently, better targeted treatments, which depend on monoclonal antibodies (mAb) that bind to specific targets on the surface of tumour cells, have been introduced. These differ from traditional treatments as they target cancer cell apoptosis by blocking oncogenic pathways and restricting angiogenesis.⁶

Many mAb have been approved by the US Food and Drug Administration (FDA).⁷ Bevacizumab (Avastin[®], Hoffmann-La-Roche) is a recombinant human immunoglobulin G (IgG1) antibody that is indicated for the treatment of many solid cancers such as metastatic breast cancer, renal carcinoma, and advanced non-small-cell lung cancer.⁸ It causes the regression of immature tumour vasculature, and inhibits

E-mail address: baljandan@iau.edu.sa

further angiogenesis by preventing the interaction of vascular endothelial growth factor-A (VEGF-A) with its receptors, and subsequent activation.⁹ However, in conjunction with its promising antineoplastic activity, patients have suffered from side effects such as hypertension, epistaxis, gastrointestinal haemorrhage, bleeding, proteinuria, and thromboembolic events.¹⁰

Recently, because of the increasing number of cases of osteonecrosis of the maxilla and mandible that have been associated with other antiresorptive (denosumab) and antiangiogenic treatments, the Committee of the American Association of Oral and Maxillofacial Surgeons (AAOMS) suggested that “bisphosphonate-related osteonecrosis of the jaw” (BRONJ) should be changed to “medication-related osteonecrosis of the jaw” (MRONJ).¹¹ Osteonecrosis of the jaw (ONJ) has been described in patients who have antitumour treatments that target VEGF-A,¹² and to our knowledge, bevacizumab-related ONJ was first reported in 2008 by Estilo et al.¹³

The effect of antiangiogenic chemotherapy on the osseointegration of titanium implants has been reported in two in-vivo studies. Al Subaie et al concluded that ranibizumab (anti-VEGF) can adversely affect bony healing and the osseointegration of titanium implants.¹⁴ An earlier study on the effect of TNP-470 (a potent inhibitor of angiogenesis) in rabbits, found that the quality of the bone:implant contact was not affected, but that the amount of newly-formed bone around the implant was reduced.¹⁵

We have investigated the effect of targeted chemotherapy with bevacizumab (Avastin[®]) on the osseointegration of titanium implants in rabbits using microcomputed tomographic (CT) and histomorphometric analyses.

Material and methods

Experimental animals and ethics approval

The study was conducted using 14 adult male New Zealand rabbits aged 6–8 months and weighing 3–4 kg. For the duration of the study they were all housed separately in stainless-steel cages under controlled conditions (25 °C, 50%–55% relative humidity, and 12-hour light/dark cycles), and had free access to food (standard rabbit pellets) and water.

Ethics approval was obtained from the review board at our institute (Approval No IRB-201602073). The study design followed ARRIVE (Animal Research: Reporting of In Vivo Experiments) guidelines, and the experimental protocol followed the National Institute of Health Guidelines (NIH Publications No. 80-23; 1996).

Study design

Animals were allocated randomly into two groups of seven each: the placebo control group and the Avastin[®] group.

Animals in the Avastin[®] group were given five doses (3 mg/kg/week) of bevacizumab intraperitoneally (Avastin[®], Hoffmann-La-Roche). To test its effect on bone formation, the treatment started at roughly the same time as the placement of implants. However, to reduce stress and the risk of death, the first dose was given two days before the operation. The next was given one week after the first dose, and the remaining three were given weekly for three weeks. The bevacizumab infusion was freshly prepared every week by dilution in normal saline. Animals in the control group were given similar treatment but the injections were all of normal saline. All animals were weighed every week and the volume of the injection adjusted accordingly (1 ml/kg).

The sample size was calculated with the help of an online calculator¹⁶ using the following assumptions: α error = 5%; power = 80%; means in the two groups (which were based on a similar study by Mair et al¹⁵) = 46.1% and 58.4%; SD = 7; and sampling ratio = 1:1. The minimum sample size required was six/group with an additional 10% to compensate for potential dropouts. The sample size/group was therefore planned to be seven.

Operation

The operations have been described in detail previously.⁴ Briefly, the animals were anaesthetised by intramuscular injection of 30 mg/kg ketamine and 5 mg/kg xylazine. After preparation of the surgical site, a 2 cm skin incision was made on the lateral surface of the hind leg, and the flat bony surface on the lateral aspect of the distal condyle exposed by blunt dissection of the muscles and reflection of the periosteum. One titanium dental implant (SICmax[®], SIC invent AG) 3.7 mm in diameter and 7.5 mm long was placed in each rabbit. Finally, the surgical sites were closed in layers with Vicryl 3/0 (Ethicon), and animals were injected with 1.5 mg/kg of diclofenac sodium and 15 mg/kg of oxytetracycline every 24 hours for three days.

The animals were killed four weeks after the operation by an overdose of pentobarbital (Narkoren[®], Merial GmbH). The femoral specimens were then collected, cleaned, and sectioned with a circular saw (1 cm proximal and 1 cm distal to the implant), and preserved in 10% formalin for subsequent microCT and histomorphometric analysis.

MicroCT analysis

Bone blocks containing the implants were scanned by microCT (SkyScan 1172). We used a high-resolution scanner (image pixel size = 27.45 μ m, source voltage = 100 kV, source current = 100(μ A), and exposure time = 1500 ms), and 3-dimensional reconstruction software (SkyScan CT-Analyser software, version 1.14) to generate 3-dimensional models and to obtain the ratio of bone volume:tissue volume (BV:TV) within the regions of interests. To reduce the effects of metal artefacts during analysis of the morphometric

variables of the bone (percentage bone:implant contact and BV:TV), we excluded four dilatations in pixel size from the surface of the implant, each dilatation equal to 27.45 μm .¹⁷

We analysed three variables from two regions of interest along the length of the implant. The first was the percentage of 3-dimensional bone:implant contact. This was taken from a ring of bone that was in direct contact with the surface of the implant, with a 1-pixel thickness of 27.45 μm after four dilatations in pixel size; the ratio of BV:TV in this ring was considered to be the percentage of 3-dimensional bone:implant contact. The second was the BV:TV–500 μm , which was a ring of bone around the implant 500 μm from the surface of the implant after four dilatations in pixel size. The third was the percentage of 2-dimensional bone:implant contact, also after four dilatations, which was obtained automatically by the software by running a 2-dimensional morphometric analysis and selecting the percentage intersection surface $i.S/\text{peripheral tissue surface TS} = i.S/\text{TS}$ (per), which was equal to the percentage of 2-dimensional bone:implant contact.

Histological analysis

After fixation in 10% formaldehyde solution, specimens were dehydrated in ascending grades of ethanol and methyl methacrylate before being embedded in a light cure acrylic resin (Technovit 7200, Kulzer GmbH). They were then cut longitudinally with a Leica SP 1600 microtome saw (Leica Biosystems) along the lateral surface of the implant to obtain the most central sections. Their thickness was reduced to roughly 30 μm with ascending grades of sandpaper, and finally polished using a microgrinding system (MetaServ 250, Buehler). Histological sections were stained with 1% toluidine then viewed with a Nikon Eclipse LV100 POL microscope. Images were captured with a Nikon DS-Fi3 camera. ImageJ software (ImageJ 1.43 Hz) was used to detect the amount of osseointegration by calculating the percentage contact between the implant and bone.

Statistical analysis

Statistical analysis was done with the help of IBM SPSS Statistics for Windows, version 20 (IBM Corp). Probabilities of less than 0.05 were considered significant. The outcome variables were tested for homogeneity of variance using Levene's test, which proved to be insignificant. For microCT, the variables tested were the percentage of 3-dimensional bone:implant contact, the percentage BV:TV, and the percentage of 2-dimensional bone:implant contact (p values were 0.096, 0.217, and 0.523, respectively). The percentage of bone:implant contact was evaluated by histomorphometric analysis (p=0.55). Study outcomes were normally distributed (skewness was within the range ± 2). Parametric analysis (independent samples *t* test) was done to calculate differences between the outcomes of the two groups.

Results

MicroCT evaluation

The qualitative assessments of the bone around the implant from the 3-dimensional microCT images for both groups are shown in Figs. 1 and 2. Table 1 shows the microCT results (after four weeks of healing) of the percentage of 3-dimensional bone:implant contact, ratio of bone volume:total volume 500 μm from the surface of the implant, and percentage of 2-dimensional bone:implant contact.

Histological evaluation

The mean value of newly-formed bone trabeculae (T) that were in direct contact with both sides of the implant (I) was observed in both groups. Coronal and apical portions of the implants showed greater contact than the middle parts because of the large marrow spaces (M) in the rabbit bone. Newly formed bone was stained lighter than original bone, and was most likely to be in areas adjacent to original cortical bone (C). The groups differed, and the bone generated around the implants in the Avastin[®] group had fewer and slimmer trabeculae than that generated in the control group. Also, the intertrabecular spaces were wider in the Avastin[®] group than in the controls (Figs. 3 and 4).

Histomorphometric evaluation

The percentage bone:implant contact was significantly higher in the control group than in the Avastin[®] group (p = 0.0001) (Table 2).

Discussion

Rabbits have previously been used to examine the action of various cytotoxic and anti-inflammatory compounds on the osseointegration of dental implants.⁴ In a rabbit's skeletal system, the distal femur and proximal tibia are appropriate insertion sites for dental implants because they can be accessed easily, and their distinct cortical and trabecular bony content support the implant.

Bevacizumab is a recombinant human mAb to VEGF-A that represses tumour angiogenesis, development, and metastasis, by preventing VEGF-A from binding to its receptor.¹⁸ In our study, treatment resulted in a lower percentages of bone:implant contact and BV:TV–500 μm . It also reduced the amount of trabecular bone, and increased trabecular separations around the implant. These findings suggest that the blocking of the VEGF-A signalling pathway, and the resulting impairment of angiogenesis by bevacizumab, may have a negative impact on the osseointegration of these implants.

Angiogenesis is the development of new capillary blood vessels that originate from a pre-existing vasculature. It

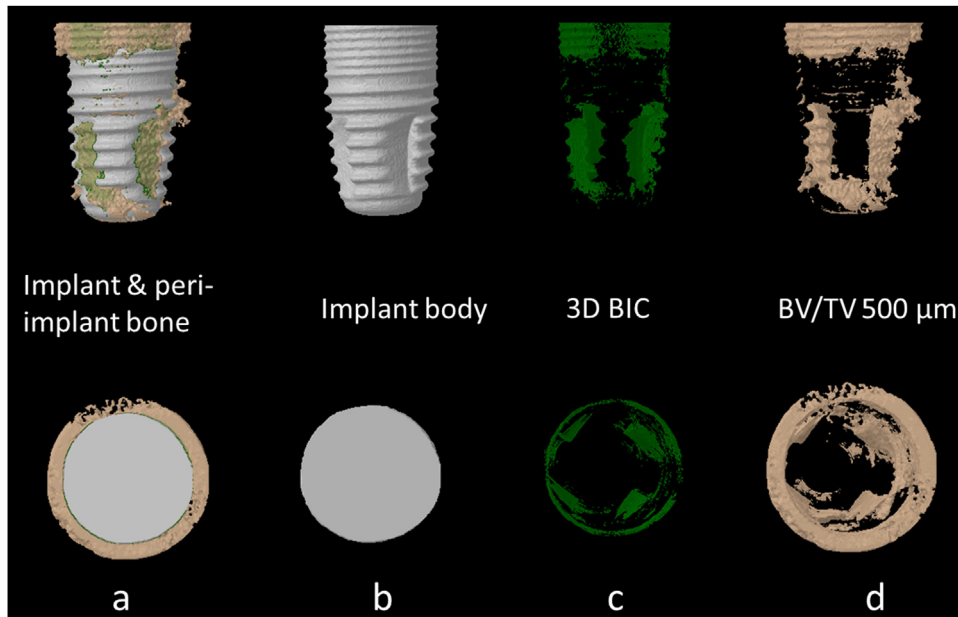


Fig. 1. Control group: 3-dimensional microcomputed tomography (CT) of the implant and surrounding bone (longitudinal and top views); (a) the implant and bone around the implant in the selected regions of interest; (b) the implant body without the bone; (c) 3-dimensional bone:implant contact after excluding the implant. (d) bone volume:tissue volume 500 μm from the surface of the implant after excluding the implant.

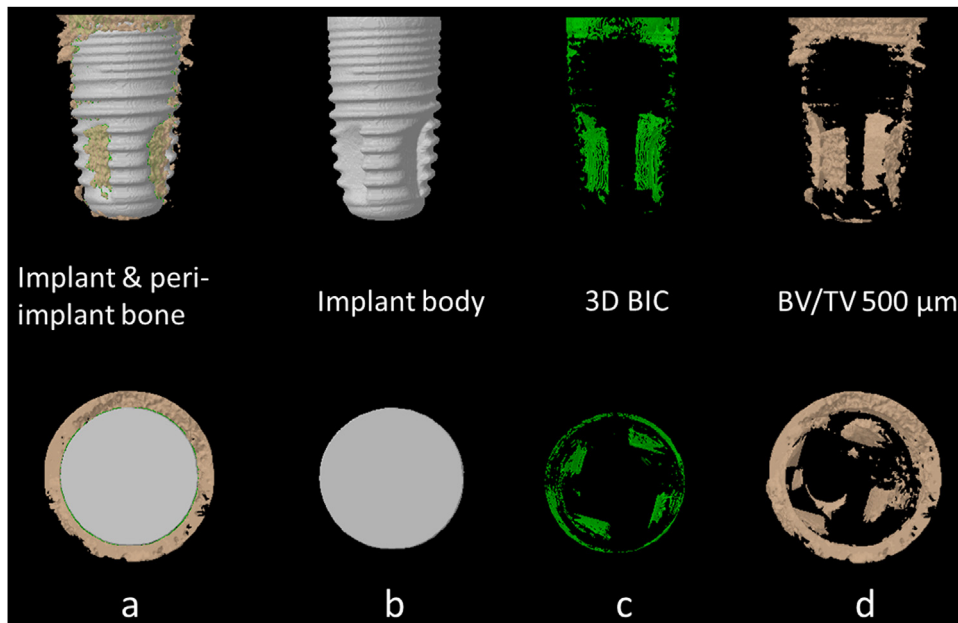


Fig. 2. Avastin[®] group: 3-dimensional microcomputed tomography (CT) of the implant and surrounding bone (longitudinal and top views); (a) the implant and surrounding bone in the selected regions of interest; (b) the implant without the bone; (c) 3-dimensional bone:implant contact after excluding the implant; (d) bone volume:tissue volume 500 μm from the surface of the implant after excluding the implant.

Table 1

Microcomputed tomographic results after four weeks of healing of the percentage 3-dimensional and 2-dimensional bone:implant contact (3D and 2D BIC), and ratio of bone volume:total volume (BV:TV) 500 μm from the surface of the implant.

Variables	Mean (SD) Avastin [®] (%)	Mean (SD) control (%)	t test (Avastin [®] cf control)	p value	Mean (95% CI) difference
3D BIC	33.76 (8.30)	43.58 (3.50)	2.884	0.014*	9.82 (2.41 to 17.24)
BV/TV 500 μm	17.22 (6.50)	20.40 (3.58)	1.110	0.289	3.17 (−3.05 to 9.40)
2D BIC	41.26 (9.81)	57.49 (7.54)	3.471	0.005*	16.23 (6.04 to 26.42)

cf = compared with.

* Significant.

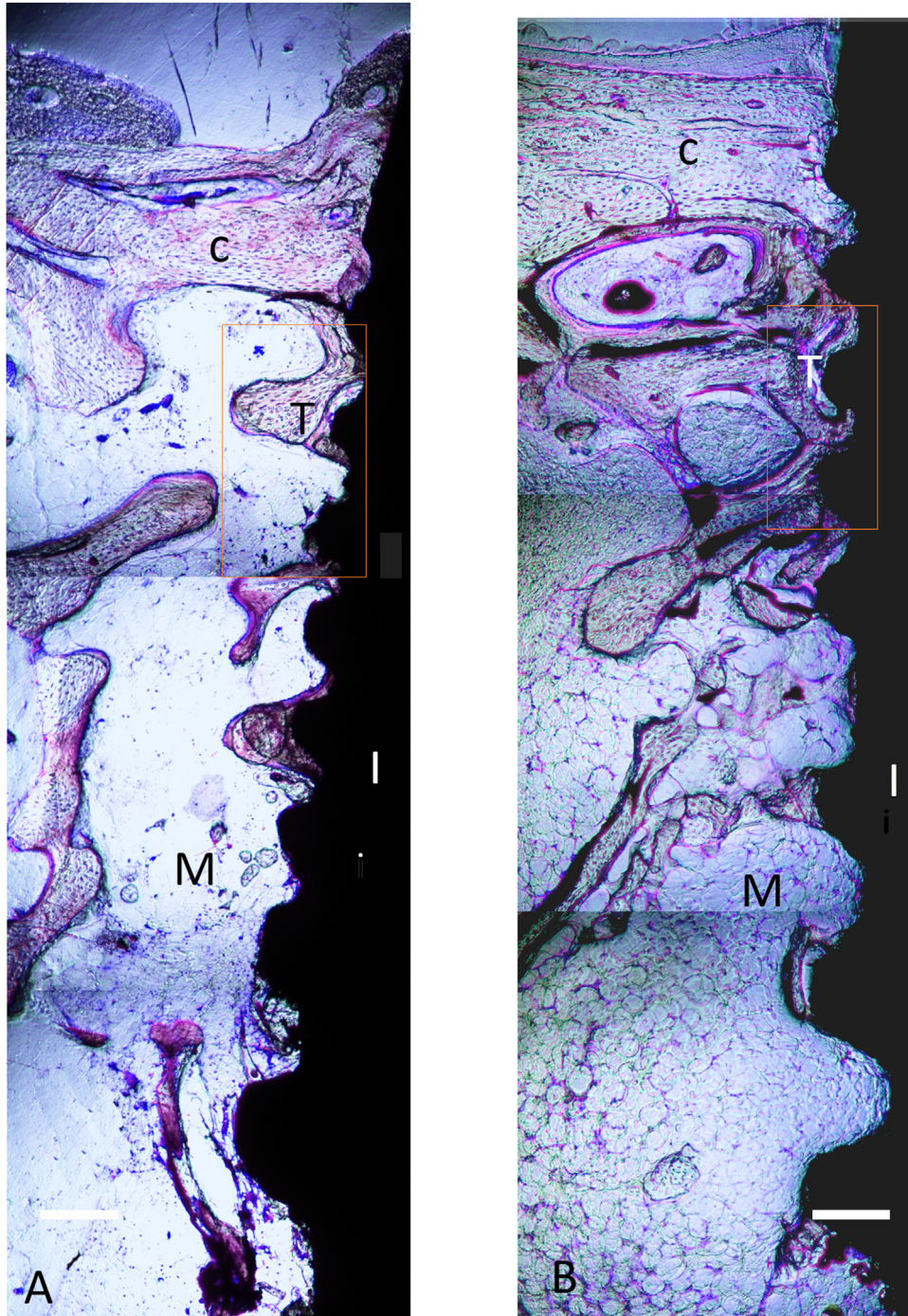


Fig. 3. Photomicrograph of histological sections: (A) Avastin[®] group, (B) control group (1% toluidine blue stain, scale bar = 0.2 mm) (T = newly-formed bone trabeculae; C = cortical bone; M = marrow spaces; I = implant).

Table 2
Histomorphometric results of percentage bone:implant contact (BIC).

Variable	Mean (SD) Avastin [®]	Mean (SD) control	<i>t</i> -test (Avastin [®] cf control)	p value	Mean (95% CI) difference
BIC (%)	25.23 (2.91)	48.26 (2.48)	12.023	0.0001	23.03 (18.34 to 27.72)

cf = compared with.

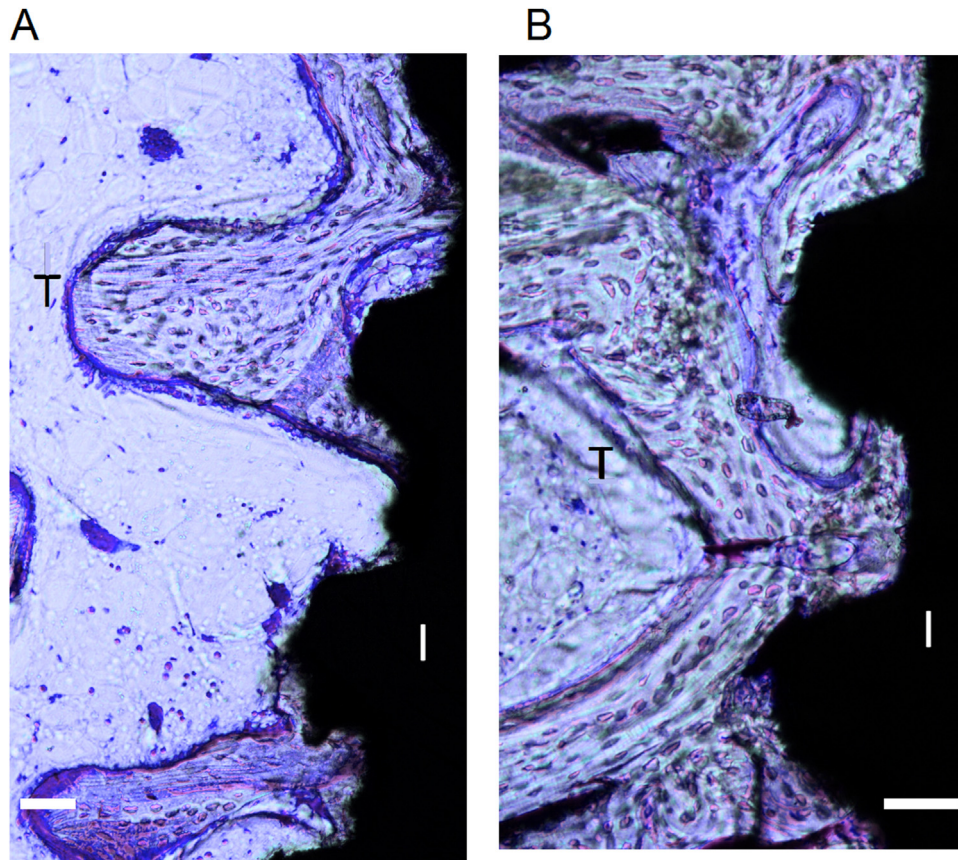


Fig. 4. Photomicrograph of histological sections: (A) Avastin[®] group, (B) control group (1% toluidine blue stain, scale bar = 0.1 mm).

is a biologically crucial step in several physiological processes including embryonic development, the regeneration of new bone after skeletal fractures, and the osseointegration of implanted prostheses.¹⁹ Endogenously, the sprouting of new blood capillaries involves a complex synchronisation between numerous biological events and growth factors such as VEGF-A, epidermal growth factor (EGF), and basic fibroblast growth factor (FGF-2). For instance, the osteoblasts and hypertrophic chondrocytes can produce VEGF-A. The binding of VEGF-A to its receptors initiates cascades of intracellular signal transduction that activate the growth and development of endothelial cells.²⁰ EGF and FGF-2 may also provoke angiogenesis by potentiating the production of VEGF.²¹

Studies have also found that factors that stimulate osteogenesis such as 1,25-dihydroxyvitamin D₃, 17 β -oestradiol, and bone morphogenetic protein-2, may regulate the expression of these angiogenic factors.^{22,23} Interestingly, Raines et al found that the microtopography and energy of the surface of titanium implants may regulate the osteoblast-induced generation of angiogenic growth factors.¹⁹

We found that bevacizumab can impair the development of bone around the implant and reduce the percentages of bone:implant contact and BV:TV–500 μ m. Our results agreed with those in other studies. In an *in vitro* study, Guang et al reported that VEGF provoked the proliferation of

osteoblasts as well as the expression and secretion of VEGF and alkaline phosphatase. In the *in vivo* part of their study, the implants that had been pre-coated with VEGF markedly improved the development of osteoblasts and endothelial cells, which suggested that inhibition of the VEGF signalling cascade may negatively affect the integration of dental implants in bone.²⁴ Notably, use of an experimental compound (TNP-470) to impair the formation of blood vessels, reduced the formation of bone around the implant, but did not affect overall contact between the implant and bone.¹⁵ TNP-470 is an antiangiogenic compound that blocks the differentiation of vascular smooth muscle cells such as fibroblasts and endothelial cells. In another study, ranibizumab, a human recombinant fragment of a mAb that constrains VEGF-A, was found to compromise bony healing and the osseointegration of dental implants in rat tibias.¹⁴

Our study has two limitations. First, there are differences between rabbits and humans in the pattern and quality of the skeletal systems so we suggest the use of larger animals in further studies. Secondly, we did not assess the long-term effects of targeted chemotherapy on the osseointegration of titanium dental implants. The effects of bevacizumab on the quality of the bone around the implants were evaluated at one time point only, but previous studies have considered this sufficient time for the angiogenesis and healing of bony defects, and for the expression of VEGF, to be clear.^{24,25}

In summary, volumetric changes in the freshly developed bone after treatment with bevacizumab, suggest that the dose given may impair the re-establishment of mineralised tissue around the implant. The pharmacological inhibition of angiogenesis may therefore have a deleterious effect on the osseointegration of titanium implants in rabbits.

Ethics statement/confirmation of patients' permission

Ethics approval was obtained from the ethical review board at our institute (Approval No IRB- 245 201602073). Patients' permission N/A.

Conflict of interest

I have no conflicts of interest.

Appendix A. Supplementary data

Supplementary data associated with this article can be found, in the online version, at <https://doi.org/10.1016/j.bjoms.2019.01.003>.

References

1. Buser D, Janner SF, Wittneben JG, et al. 10-year survival and success rates of 511 titanium implants with a sandblasted and acid-etched surface: a retrospective study in 303 partially edentulous patients. *Clin Implant Dent Relat Res* 2012;**14**:839–51.
2. Prasanna PG, Stone HB, Wong RS, et al. Normal tissue protection for improving radiotherapy. Where are the gaps? *Transl Cancer Res* 2012;**1**:35–48.
3. Lobato-Mendizábal E, Ruiz-Argüelles GJ. Leukemia and malnutrition. II. The magnitude of maintenance chemotherapy as a prognostic factor in the survival of patients with standard-risk acute lymphoblastic leukemia. *Rev Invest Clin* 1990;**42**:81–7. In Spanish.
4. Al-Mahalawy H, Marei HF, Abuohashish H, et al. Effects of cisplatin chemotherapy on the osseointegration of titanium implants. *J Craniomaxillofac Surg* 2016;**44**:337–46.
5. Xu G, McLeod HL. Strategies for enzyme/prodrug cancer therapy. *Clin Cancer Res* 2001;**7**:3314–24.
6. Schlaeppli JM, Wood JM. Targeting vascular endothelial growth factor (VEGF) for anti-tumor therapy, by anti-VEGF neutralizing monoclonal antibodies or by VEGF receptor tyrosine-kinase inhibitors. *Cancer Metastasis Rev* 1999;**18**:473–81.
7. Highlights of prescribing information. Rituximab. Initial US approval: 1997. Available from URL: https://www.accessdata.fda.gov/drugsatfda_docs/label/2018/103705s5450lbl.pdf (last accessed 30 December 2018).
8. Ferrara N, Hillan KJ, Gerber HP, et al. Discovery and development of bevacizumab, an anti-VEGF antibody for treating cancer. *Nat Rev Drug Discov* 2004;**3**:391–400.
9. Ferrara N, Hillan KJ, Novotny W. Bevacizumab (Avastin), a humanized anti-VEGF monoclonal antibody for cancer therapy. *Biochem Biophys Res Commun* 2005;**333**:328–35.
10. Geiger-Gritsch S, Stollenwerk B, Miksad R, et al. Safety of bevacizumab in patients with advanced cancer: a meta-analysis of randomized controlled trials. *Oncologist* 2010;**15**:1179–91.
11. Ruggiero SL, Dodson TB, Fantasia J, et al. American Association of Oral and Maxillofacial Surgeons position paper on medication-related osteonecrosis of the jaw—2014 update. *J Oral Maxillofac Surg* 2014;**72**:1938–56.
12. Van Poznak C. Osteonecrosis of the jaw and bevacizumab therapy. *Breast Cancer Res Treat* 2010;**122**:189–91.
13. Estilo CL, Fornier M, Farooki A, et al. Osteonecrosis of the jaw related to bevacizumab. *J Clin Oncol* 2008;**26**:4037–8.
14. Al Subaie AE, Eimar H, Abdallah MN, et al. Anti-VEGFs hinder bone healing and implant osseointegration in rat tibiae. *J Clin Periodontol* 2015;**42**:688–96.
15. Mair B, Fuerst G, Kubitzky P, et al. The anti-angiogenic substance TNP-470 impairs peri-implant bone formation: a pilot study in the rabbit metaphysis model. *Clin Oral Implants Res* 2007;**18**:370–5.
16. Online calculator. Available from URL: <http://powerandsamplesize.com/Calculators/Compare-2-Means/2-Sample-Equality> (last accessed 3 January 2019).
17. Song JW, Cha JY, Bechtold TE, et al. Influence of peri-implant artifacts on bone morphometric analysis with micro-computed tomography. *Int J Oral Maxillofac Implants* 2013;**28**:519–25.
18. Spicer J, Irshad S, Ang JE, et al. A phase I study of afatinib combined with paclitaxel and bevacizumab in patients with advanced solid tumors. *Cancer Chemother Pharmacol* 2017;**79**:17–27.
19. Raines AL, Olivares-Navarrete R, Wieland M, et al. Regulation of angiogenesis during osseointegration by titanium surface microstructure and energy. *Biomaterials* 2010;**31**:4909–17.
20. Stoelcker B, Echtenacher B, Weich HA, et al. VEGF/Flk-1 interaction, a requirement for malignant ascites recurrence. *J Interferon Cytokine Res* 2000;**20**:511–7.
21. Ravindranath N, Wion D, Brachet P, et al. Epidermal growth factor modulates the expression of vascular endothelial growth factor in the human prostate. *J Androl* 2001;**22**:432–43.
22. St-Arnaud R. The direct role of vitamin D on bone homeostasis. *Arch Biochem Biophys* 2008;**473**:225–30.
23. Fiorellini JP, Chen PK, Nevins M, et al. A retrospective study of dental implants in diabetic patients. *Int J Periodontics Restorative Dent* 2000;**20**:366–73.
24. Guang M, Huang B, Yao Y, et al. Effects of vascular endothelial growth factor on osteoblasts around dental implants in vitro and in vivo. *J Oral Sci* 2017;**59**:215–23.
25. Dimitriou R, Tsiridis E, Giannoudis PV. Current concepts of molecular aspects of bone healing. *Injury* 2005;**36**:1392–404.